

Aligning Attention Distribution to Information Flow for Hallucination Mitigation in Large Vision-Language Models

Jianfei Zhao^{1,2}, Feng Zhang¹, Xin Sun¹, Chong Feng^{1,3,*},

¹School of Computer Science and Technology, Beijing Institute of Technology, Beijing, China,

²Zhongguancun Academy, Beijing, China,

³Southeast Academy of Information Technology, Beijing Institute of Technology, Fujian, China,

Abstract

Due to the unidirectional masking mechanism, Decoder-Only models propagate information from left to right. LVLMs (Large Vision-Language Models) follow the same architecture, with visual information gradually integrated into semantic representations during forward propagation. Through systematic analysis, we observe that over 80% of the visual information is absorbed into the semantic representations. However, the model’s attention still predominantly focuses on the visual representations. This misalignment between the attention distribution and the actual information flow undermines the model’s visual understanding ability and contributes to hallucinations. To address this issue, we enhance the model’s visual understanding by leveraging the core information embedded in semantic representations. Specifically, we identify attention heads that focus on core semantic representations based on their attention distributions. Then, through a two-stage optimization paradigm, we propagate the advantages of these attention heads across the entire model, aligning the attention distribution with the actual information flow. We evaluate our method on three image captioning benchmarks using five different LVLMs, demonstrating its effectiveness in significantly reducing hallucinations. Further experiments reveal a trade-off between reduced hallucinations and richer details. Notably, our method allows for manual adjustment of the model’s conservativeness, enabling flexible control to meet diverse real-world requirements. Code will be released once accepted.

1 Introduction

Large Vision-Language Models (LVLMs) (Liu et al., 2024c; Dai et al., 2023; Bai et al., 2023) integrate Large Language Models (LLMs) with visual encoders, aligning the extracted visual features

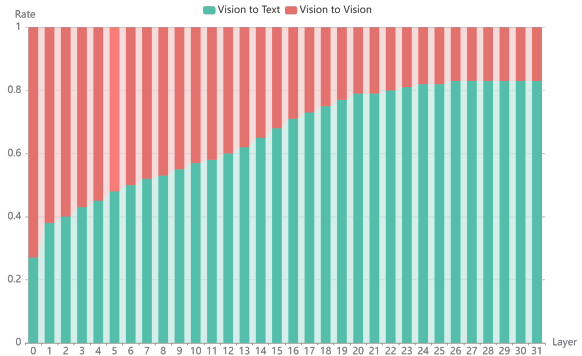


Figure 1: Visual information flow in the image captioning task on LLaVA-1.5. *Vision to Vision* and *Vision to Text* respectively denote the visual features’ contributions to the visual representations and semantic representations.

with the semantic space of the LLMs to enable comprehensive understanding of visual content. However, they often suffer from the problem of hallucination (Ji et al., 2023; Liu et al., 2024b), where the models may generate content that is inconsistent with the visual evidence, thereby severely undermining their reliability in real-world scenarios.

Recent studies have explored methods to mitigate hallucinations in LVLMs. Some works attribute hallucinations to the influence of language priors (Leng et al., 2024; Zhang et al., 2025), proposing contrastive decoding-based methods to suppress language priors. However, they do not explicitly enhance the model’s visual understanding capabilities. Other studies argue that LVLMs exhibit biased mechanisms in visual attention distribution (Yin et al., 2025; Kang et al., 2025; He et al., 2024), and propose optimizations such as increasing the relative weight of key visual tokens. In this work, however, we point out that these approaches make suboptimal adjustments to the information flow, as they overlook the influence of information aggregation.

In fact, the unidirectional masked generation pro-

*Corresponding Autor: fengchong@bit.edu.cn

cess in Transformer-based models can be regarded as a form of information flow (Vaswani et al., 2017), where information from earlier tokens in the input or generated sequence flows toward later tokens. Since LVLMs adopt this architecture, their understanding of visual content can be modeled as a process in which visual information flows into the semantic representations (since visual tokens are positioned before the textual tokens). Based on this perspective, we follow the Attention Rollout (Abnar and Zuidema, 2020) to conduct an in-depth analysis of information flow within LVLMs. The visualization results are shown in Fig. 1.

Specifically, we use $F_{i,j}^l$ to represent the contributions of the i -th input embedding to the j -th representation in layer l . Considering the residual connection in the forward propagation, we formulate the recursive relation as $F^l = (I + W_{attn})/2 \cdot F^{l-1}$, where W_{attn} is the attention weight after average pooling across multi-heads. The contributions of each input embedding were normalized to 1 across all representations. We perform layer-wise quantification of visual embeddings’ contributions to the visual and semantic representations, respectively.

As shown in the visualization, visual information progressively flows into semantic representations across layers. In the final layers, more than 80% of the visual information is integrated into the semantic representations. This indicates that, **during the forward pass of the LVLMs, visual information is gradually encoded into the semantic representations**. While prior works largely concentrate on optimizing attention allocation to visual features, they neglect the critical insight that essential information has already been integrated into semantic representations, where attention refinement may be more impactful.

To further validate this insight, we mask all visual representations and compare the consistency between the logits distribution of the vision-masked input and that of the regular (unmasked) input, as illustrated in Fig. 2. We observe that applying masking to visual representations starting from earlier layers leads to significant deviations in the model’s outputs, whereas masking from later layers has minimal impact on the final outputs. This finding further supports our view that visual information has already been integrated into the semantic representations in the later layers.

Building upon the above findings, as the number of layers increases, textual representations progressively integrate more visual information and

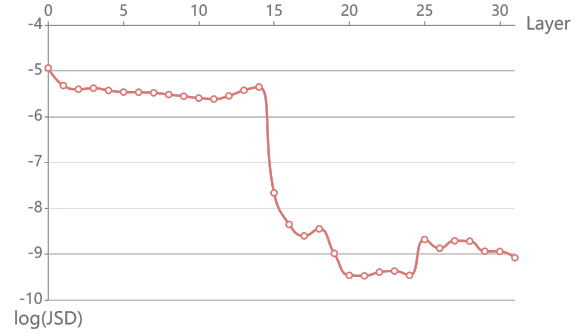


Figure 2: Jensen-Shannon divergence (JSD) between the regular and vision-masked logits distribution. $layer=l$ represents the application of masking vision features starting from the l -th layer. Lower $logJSD$ denotes higher consistency between two distributions. The generation context is *The image depicts*.

thus play an increasingly important role. Consequently, LVLMs should place greater attention on these integrated representations. To investigate this, we statistically analyze the attention allocation between semantic representations and others at each layer, as illustrated in Fig. 3. **The model’s attention to semantic representations is significantly lower** than expected, accounting for only about one-fifth of the total attention. We attribute this phenomenon to the nature of supervision in LVLm training, which is primarily driven by soft supervision from end-to-end data and lacks explicit guidance on attention allocation. Therefore, we argue that **the misalignment between the attention distribution and the visual information flow is a major contributing factor to hallucinations**, as the model does not sufficiently attend to regions enriched with visual information.

To address the aforementioned challenge, we propose SEVI (Semantic-Enhanced Visual Interpretation), a novel training-free approach that augments the model’s attention to those semantic representations that have absorbed visual information. Furtherly, we encourage the model to focus on the most meaningful representations in order to reduce the occurrence of hallucinations. Several studies (Wang et al., 2023; Xiao et al., 2024) have revealed that contextual information tends to spontaneously concentrate in some tokens, forming anchor tokens that encapsulate key information. These tokens are typically characterized by receiving disproportionately high attention, as shown in Fig. 4. Therefore, our method focuses the model’s attention on these core semantic representations at higher lay-

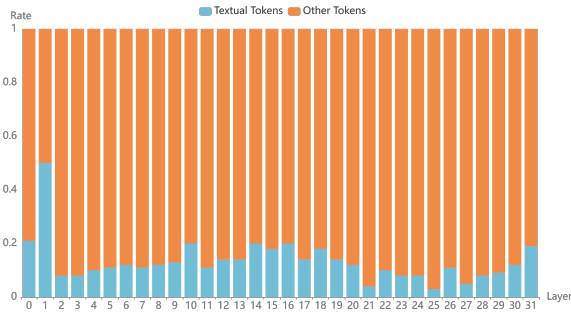


Figure 3: Attention distribution between textual tokens and all other tokens, obtained by averaging across all attention heads.

ers where information integration and aggregation occur. The key visual information contained within these representations provides more effective guidance for the model’s understanding of visual inputs, thereby mitigating hallucination. Specifically, we identify superior attention heads within the multi-head attention mechanism—those that attend to core semantic representations—and use their attention distribution as the target distribution to guide the optimization of the overall model attention. To achieve this, we design a two-stage attention refinement paradigm, incorporating a smoothing mechanism to ensure stable performance improvements.

We evaluate the effectiveness of our method in mitigating hallucinations by testing it with five LVLMs: InstructBLIP (Dai et al., 2023), LLaVA-1.5 (Liu et al., 2024c), LLaVA-Next (Liu et al., 2024d), Qwen2-VL-Instruct (Wang et al., 2024c), and Qwen2.5-VL-Instruct (Bai et al., 2025), on three image captioning benchmarks: CHAIR (Rohrbach et al., 2018), AMBER (Wang et al., 2024b), and DetailCaps (Ye et al., 2025). Experimental results show that our approach significantly reduces hallucinations while supporting manual adjustment of the model’s conservativeness, enabling a flexible trade-off between cautious outputs (fewer hallucinations) and comprehensive descriptions (richer details).

Our main contributions are as follows:

- We reveal that visual information is indeed integrated into semantic representations. However, the model’s attention allocation does not align with this flow pattern, as it continues to focus more on visual representations.
- We enhance the visual understanding capabilities of LVLMs by leveraging semantic representations. Specifically, we guide the model’s

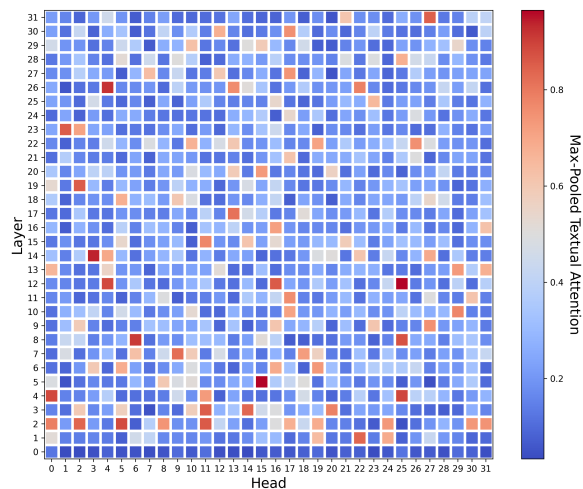


Figure 4: Semantic attention distribution of LLaVA-1.5 during image description. We compute the proportion of peak attention within the semantic representations relative to the entire set of textual tokens.

attention toward core semantic representations through a two-stage optimization paradigm, effectively reducing hallucinations.

- We evaluate our method on the image captioning task, demonstrating its effectiveness in significantly reducing hallucinations across three benchmark datasets and five LVLMs. We observe a trade-off between reducing hallucinations and preserving detail, with our method enabling controllable conservativeness for task-specific needs.

2 Related Work

Various approaches have been proposed to mitigate hallucinations in LVLMs, such as improving training data quality (Liu et al., 2024a; Sun et al., 2024; Gunjal et al., 2024) or designing specific data formats (Chen et al., 2025; Hu et al., 2023; Zhai et al., 2024) to enhance model reliability. However, these training-based methods often suffer from limited scalability.

In recent years, the rapid evolution of LVLMB backbones has brought increasing attention to training-free methods. Early approaches (Yin et al., 2024; Wang et al., 2024a; Zhou et al., 2024) primarily relied on post-processing techniques to correct hallucinated content after generation. However, the complexity of such pipelines and their dependence on external modules limited their practical usability. Researchers have since shifted focus toward investigating the root causes of hallucinations, exploring

targeted optimizations in both the decoding strategies and the decoding processes. Some methods (Leng et al., 2024; Wang et al., 2024d; Zhang et al., 2025; Zhao et al., 2025) apply contrastive decoding algorithms to refine the logits, thereby reducing the likelihood of hallucination-related tokens. While these approaches improve the expressiveness of the model and enhance the transfer of visual information into textual form, they do not strengthen the model’s intrinsic cross-modal understanding. Other works have proposed enhancements to the attention mechanism, such as correcting visual positional bias (Li et al., 2025; Zhu et al., 2025), directly boosting visual attention (Zhu et al., 2024; He et al., 2024), or redistributing attention weights (Kang et al., 2025; Yin et al., 2025). However, these methods primarily concentrate on visual attention and overlook the vision-integrated semantic representation.

In contrast to these approaches, we analyze the information flow between the visual and textual modalities in LVLMs and focus the model’s attention on key information within semantic representations, thereby reducing hallucinations more effectively.

3 Preliminary

LVLMs consist of a visual encoder and an LLM backbone. High-dimensional features extracted by the visual encoder are concatenated with textual embeddings and jointly fed into the LLM. Subsequently, the visual and semantic features undergo cross-modal interaction through the Self-Attention layers within the LLM. The cross-modal interaction in layer l simplified as $\Delta X^l = \text{softmax}(W)X^l$, where $X^l = [X_V^l : X_T^l]$ denotes the hidden states of visual features X_V^l and semantic features X_T^l . $W \in \mathbb{R}^{H \times L \times L}$ is the attention weights, H is the number of attention head and L is the model’s context length.

When generating the $(j+1)$ -th token, the LVLM’s attention to feature X_i^l at layer l is quantified by the weight value $W_{i,j}$. A larger $W_{i,j}$ indicates that the model’s current layer relies more heavily on the information from X_i^l when determining the generated content. Therefore, we can intuitively infer that more important features X_i^l should generally correspond to larger attention weights $W_{i,j}$.

4 Method

We attribute the occurrence of hallucinations to a misalignment between the attention allocation of LVLMs and the underlying information flow. To address this, we enhance the visual interpretation capabilities of LVLMs by leveraging semantic representations that encapsulate visual information. We first identify superior attention heads that focus on core semantic representations, and then propagate their strengths to other heads through a two-stage optimization paradigm, as illustrated in Fig. 5.

4.1 Attention allocation Alignment

Considering that visual information is progressively integrated into semantic representations through forward propagation—and that only a few of these representations aggregate key information—an intuitive approach is to increase the model’s attention to these core semantic representations in the later layers. However, rigidly modifying the model’s attention distribution may disrupt its inherent latent features, potentially resulting in suboptimal performance.

In multi-head attention mechanisms, attention heads naturally diversify after training, forming a heterogeneous and specialized structure (Vaswani et al., 2017). Accordingly, we identify superior attention heads that attend to core semantic representations and transfer their attention patterns to other heads, leading to a global refinement of the model’s attention distribution. Specifically, at each layer, we calculate the attention weight of each head with respect to the semantic representations. We then identify those heads that allocate more than 50% of their attention to semantic representations:

$$h \in \begin{cases} H_S & \text{if } \sum W_S^h > \sum W_O^h \\ H_O & \text{if } \sum W_S^h \leq \sum W_O^h \end{cases} \quad (1)$$

H_S denotes the set of heads that focus more on semantic representations, whereas H_O denotes other heads. H_S are further categorized based on their attention distributions into *Core Semantic Heads* (H_{S_c}), which focus on core semantic representations, and *Global Semantic Heads* (H_{S_g}), which fail to effectively attend to them:

$$h \in \begin{cases} H_{S_c} & \text{if } \max \bar{W}_S^h > \kappa \\ H_{S_g} & \text{if } \max \bar{W}_S^h \leq \kappa \end{cases} \quad (2)$$

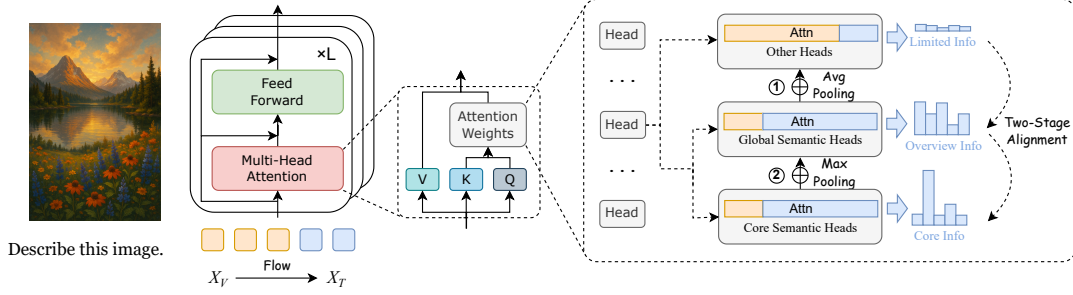


Figure 5: The diagram of our method. We first categorize attention heads based on their focus on semantic representations into semantic heads and other heads. Semantic heads are further divided into core semantic heads and global semantic heads, depending on whether they attend to core semantic representations. We then align the model’s attention distribution with the core semantic heads through a two-stage optimization process.

where κ is a hyperparameter. We then take core semantic heads to construct a target distribution to optimize the model’s attention allocation.

To ensure stable information integration within the model, we propose a two-stage feature optimization paradigm that more naturally guides the model’s understanding of visual information.

In the first stage, we use the global semantic heads to guide the other heads, aligning the model’s attention transition to semantic representations and harmonizing with the visual information flow. In the second stage, we leverage the core semantic heads to guide the global semantic heads, encouraging the model to concentrate more on critical information and thereby suppressing hallucinations.

The model’s internal attention is then optimized through a two-stage refinement process. During this process, we construct the guidance across attention heads by performing a weighted summation of their attention weights, and incorporate smoothing to enhance the stability of feature representations.

$$\hat{W}^h = \frac{W^h + \omega W'}{1 + \omega} \quad (3)$$

where \hat{W}^h denotes the optimized attention weights of head h , W' represents the target weight distribution derived from superior heads, and ω is a hyperparameter that controls the extent of the modification.

We first use global semantic heads to guide other heads, aiming to align the model’s attention distribution with the flow of visual information. To this end, we apply average pooling across global semantic heads to construct the target attention distribution. Subsequently, we use core semantic heads to guide the global semantic heads, with the goal

of enhancing the model’s focus on critical information. Here, we employ max pooling across core semantic heads to form the corresponding target distribution.

$$\begin{aligned} \hat{W}_O^h &= \frac{W_O^h + \omega \cdot \text{avg} W_{S_g}^h}{1 + \omega}, \\ \hat{W}_{S_g}^h &= \frac{W_{S_g}^h + \omega \cdot \text{max} W_{S_c}^h}{1 + \omega} \end{aligned} \quad (4)$$

4.2 Mitigating Aggravated Language priors

We optimize the model’s attention allocation to align with the flow pattern of visual information, which ultimately results in increased attention to semantic representations. However, while semantic representations incorporate visual information, they also inherently contain their own contextual features. As a result, increasing the model’s reliance on semantic representations will exacerbate the issue of language priors (Leng et al., 2024; Wu et al., 2022).

To address this issue, we use the CICD method (Zhao et al., 2025) to eliminate language priors while preserving visual information. CICD uses the cross-images consistency of language priors to identify detrimental priors and mitigate them by contrastive decoding:

$$\begin{aligned} \logit(y_t | v, x, y_{<t}) &= (1 + \alpha) \logit_{\theta}(y_t | v, x, y_{<t}) \\ &\quad - \alpha \logit_{\theta}(y_t | v', x, y_{<t}) \end{aligned} \quad (5)$$

where \logit_{θ} is the logit distribution after attention allocation alignment and \logit_{θ} is the regular logit distribution with a distinct image v' . α is defined as follows:

$$\alpha = 1 - \log_{10}(\text{JSD}(\logit_{\theta}; \logit_{\theta})) \quad (6)$$

MaxLen	Method	LLaVA-1.5			InstructBLIP			LLaVA-1.5-13B		
		CHAIRs↓	CHAIRi↓	Recall↑	CHAIRs↓	CHAIRi↓	Recall↑	CHAIRs↓	CHAIRi↓	Recall↑
64	Regular	24.4	8.9	56.6	35.6	13.2	56.4	24.0	7.8	56.5
	VCD	25.0	8.3	59.0	32.2	10.3	60.6	23.4	7.5	59.4
	ICD	23.2	8.1	58.4	29.8	9.8	60.6	18.8	6.6	58.4
	IBD	21.2	6.9	58.8	<u>27.8</u>	9.2	60.3	22.4	7.1	59.7
	VAR	25.2	8.6	55.3	-	-	-	25.8	8.5	56.3
	VAF	26.2	9.3	56.6	32.0	12.0	55.3	23.2	8.0	57.6
	DeFG	22.4	7.2	58.2	32.4	11.0	59.4	22.4	6.9	<u>59.6</u>
	CICD	<u>18.0</u>	6.1	59.6	23.8	7.7	62.2	20.4	6.6	59.4
	SEVI _{Balanced}	18.8	<u>5.5</u>	<u>59.5</u>	<u>27.8</u>	<u>8.8</u>	<u>60.9</u>	<u>17.8</u>	<u>5.5</u>	57.6
	SEVI _{Focused}	14.8	4.7	54.1	15.4	5.9	50.9	13.4	4.5	54.4
512	Regular	54.6	16.4	72.6	62.6	19.5	66.9	58.8	17.0	73.4
	VCD	59.8	17.8	75.6	64.8	18.8	71.9	60.2	16.4	76.9
	ICD	57.0	15.0	74.6	59.0	17.1	69.2	55.0	14.5	<u>76.4</u>
	IBD	57.6	16.5	74.2	57.6	15.7	70.8	50.6	14.3	76.1
	VAR	60.0	18.3	72.6	-	-	-	54.8	15.3	73.8
	VAF	58.8	19.0	71.3	58.6	17.8	66.9	57.2	16.2	73.7
	DeFG	57.4	16.3	<u>75.5</u>	59.0	17.7	<u>71.5</u>	51.8	14.2	75.5
	CICD	43.8	11.7	75.0	49.8	13.7	70.3	44.4	12.9	76.0
	SEVI _{Balanced}	34.8	<u>9.0</u>	68.3	<u>41.0</u>	12.4	67.1	<u>28.6</u>	8.4	68.7
	SEVI _{Focused}	17.8	5.5	56.9	18.8	8.4	51.6	15.0	5.1	55.6

Table 1: Results on CHAIR. SEVI_{Balanced} and SEVI_{Focused} represent our method operating in the *Balanced* and *Focused* mode, respectively. **MaxLen** denotes the maximum generation length.

where $JSD(\cdot; \cdot)$ represents Jensen-Shannon Divergence.

5 Experiments

5.1 Experiment Setting

Due to space constraints, we present only the key aspects of our experimental setup here. Detailed settings can be found in Sec. A.

Implementation Details Our method guides the model to focus on core information, thereby reducing the occurrence of hallucinations. In practice, we observe a trade-off between hallucination suppression and the richness of generated details, influenced by the model’s degree of attentional focus. To address this, we introduce hyperparameters to control the model’s focus on core information. Based on empirical observations, we design two sets of hyperparameter configurations: (1) *Focused* mode that aggressively minimizes hallucinations, and (2) *Balanced* mode that strikes a compromise between detail retention and hallucination reduction. Specifically, the Focused mode optimizes attention distribution starting from the 5th layer with $\omega = 4$, while the Balanced mode begins from the 9th layer with $\omega = 0.5$.

In addition, we set the parameter κ in Eq. 2 to 0.2. Further details are discussed in Appendix.

A.3. We employ sampling decoding for the next-token prediction with default settings. All experiments are performed on a single NVIDIA A800 40G GPU.

Benchmarks We evaluate the performance of our method across three widely adopted multimodal hallucination benchmarks on the image captioning task. These include CHAIR (Rohrbach et al., 2018), DetailCaps (Ye et al., 2025), and AMBER (Wang et al., 2024b).

Evaluated LLMs To examine the generalizability of our approach, we apply it to five LLMs drawn from three representative model families: InstructBLIP (Dai et al., 2023); two models from the LLaVA family (LLaVA-1.5 (Liu et al., 2024c) and LLaVA-Next (Liu et al., 2024d)); and two from the Qwen series (Qwen2-VL-Instruct (Wang et al., 2024c) and Qwen2.5-VL-Instruct (Bai et al., 2025)). All models are tested at the 7B parameter scale unless explicitly noted otherwise.

Baselines We conduct a comparison between our method and several SOTA de-hallucination techniques: VCD (Leng et al., 2024), ICD (Wang et al., 2024d), IBD (Zhu et al., 2024), VAR (Kang et al., 2025), VAF (Yin et al., 2025), DeFG (Zhang et al., 2025), and CICD (Zhao et al., 2025).

Method	LLaVA-1.5			InstructBLIP		
	CAPTUR \uparrow	CHAIRs \downarrow	CHAIRi \downarrow	CAPTURE \uparrow	CHAIRs \downarrow	CHAIRi \downarrow
Regular	52.60	55.7	17.4	52.99	58.6	18.0
VCD	52.91	55.7	16.8	53.20	59.6	18.9
ICD	52.82	53.9	16.6	53.24	55.7	16.7
IBD	52.48	54.1	15.8	54.14	56.4	15.5
VAR	52.98	55.1	17.1	52.63	55.9	16.9
VAF	52.36	55.6	18.1	52.63	55.9	16.9
DeFG	52.72	55.7	16.6	53.06	59.1	17.4
CICD	<u>55.80</u>	45.6	13.1	<u>54.20</u>	45.7	13.2
SEVI _{Balanced}	53.73	<u>31.9</u>	<u>8.8</u>	53.33	<u>38.0</u>	<u>12.8</u>
SEVI _{Focused}	58.00	19.3	6.1	56.89	18.3	8.2

Table 2: Results on the COCO subset of DetailCaps. The maximum generation length is 512.

Method	LLaVA-1.5				InstructBLIP			
	CHAIR \downarrow	Cover \uparrow	Hal \downarrow	Cog \downarrow	CHAIR \downarrow	Cover \uparrow	Hal \downarrow	Cog \downarrow
Regular	11.6	49.7	47.7	4.4	12.4	51.9	52.4	5.0
VCD	9.8	51.2	43.8	4.4	9.9	54.0	44.6	4.2
ICD	8.8	<u>51.2</u>	38.7	4.1	9.8	53.9	46.7	5.1
IBD	9.8	50.5	42.2	4.4	9.0	56.1	45.1	4.6
VAR	11.7	<u>51.2</u>	48.5	4.8	-	-	-	-
VAF	11.3	50.2	48.6	4.3	11.5	51.8	50.1	5.1
DeFG	9.1	50.7	39.9	4.1	9.7	<u>54.1</u>	44.5	5.2
CICD	6.6	52.7	34.8	2.2	<u>7.1</u>	53.6	35.0	2.3
SEVI _{Balanced}	5.6	48.6	<u>27.6</u>	<u>1.7</u>	6.0	51	<u>28.5</u>	<u>1.6</u>
SEVI _{Focused}	<u>6.1</u>	42.3	20.2	0.8	7.7	42.8	24.9	1.2

Table 3: Results on AMBER. The maximum generation length is 512.

5.2 Main Results

Results on CHAIR CHAIR is a benchmark designed to detect object hallucinations in image captions, relying on human annotations to provide reliable ground truth. Following common practice, we conduct experiments with maximum sequence lengths set to 64 and 512, respectively. The results are shown in Fig. 1. Our method effectively reduces hallucinations by guiding the model’s attention toward key information, achieving particularly low hallucination rates under the focused mode. However, we observe that when the model concentrates on critical information, it tends to become more conservative, as reflected by a slight drop

in recall. In contrast, the balanced mode allows the model to capture more details while still maintaining a low hallucination rate, resulting in the best overall performance. In addition, our method yields the most pronounced improvement on the 13B model relative to the 7B model, indicating its effectiveness in harnessing the latent capacity of larger models for visual understanding.

Results on DetailCaps DetailCaps evaluates the correctness of captions in terms of objects, attributes, and relationships, incorporating both exact-match and soft-match metrics. The experimental results are presented in Tab. 2. Our method outperforms existing approaches in both hallucina-

Method	LLaVA-next			Qwen2-VL-Instruct			Qwen2.5-VL-Instruct		
	Cs↓	Ci↓	R↑	Cs↓	Ci↓	R↑	Cs↓	Ci↓	R↑
Regular	32.2	11.0	56.4	30.2	8.3	53.1	28.6	9.3	56.0
SEVI _{Balanced}	25.8	9.3	49	20.2	5.3	54.3	22.2	7.0	53.9
SEVI _{Focused}	20.8	9.9	37.8	18.8	7.0	41.9	16.4	7.1	39.2

Table 4: Results CHAIR with more LVLMs. The maximum generation length is 128.

Setting	LLaVA-1.5		InstructBLIP	
	Cs↓	Ci↓	Cs↓	Ci↓
Regular	54.6	16.4	62.6	19.5
w/o CICD	38.6	13.9	44.4	20.3
w/o Core Heads	39.0	9.7	45	13.3
w/o Global Heads	22.2	7.0	23.2	11.6
SEVI _{Focused}	17.8	5.5	18.8	8.4

Table 5: Ablation study on CHAIR with *Focused* mode.

tion rate and overall caption correctness. Moreover, the focused mode achieves a higher CPAURE score, indicating not only a lower incidence of hallucinations but also greater accuracy in the described content. This highlights the practical value of our approach for real-world applications.

Results on AMBER AMBER carefully selects high-quality images to construct its benchmark and provides a more fine-grained evaluation of object hallucinations. The experimental results are shown in Tab. 3. Our method achieves a significantly lower hallucination rate while maintaining a comparable Cover score to other approaches, resulting in the best overall performance.

5.3 Effectiveness on more LVLMs

We evaluated our method on several state-of-the-art LVLMs, with the experimental results presented in Tab. 4. Across these models, our method continues to demonstrate strong hallucination suppression capabilities, with both modes exhibiting their expected effectiveness. These results validate the excellent generalization ability of our approach and highlight its practical potential as a training-free solution.

5.4 Ablation Study

Through a two-stage optimization paradigm, we reallocate the model’s attention toward key information, encouraging it to focus on the core content of the image and thereby reducing hallucinations. In addition, we employ the CICD method to address the issue of language priors that aggravate when the model over-focuses on semantic representations. We conduct ablation studies on these three components, with the results presented in Tab. 5. The core semantic heads play a pivotal role in guiding the model’s focus, and removing them in the ablation study leads to a noticeable increase in hallucination rate. The global semantic heads help modulate the cross-modal attention distribution, aligning it with the flow of visual information, which also contributes significantly to hallucination reduction. The combination of both components has a synergistic effect, and incorporating the CICD method to mitigate language priors, amplified by overattending to semantic representations, further enhances the performance of the model. The experimental results confirm the effectiveness and soundness of our method’s design, highlighting the value of each component.

6 Conclusion

We systematically analyze the information flow in LVLMs and verify that visual information is indeed integrated into the semantic representations. However, the model’s attention remains predominantly focused on the visual representation. This inconsistency impairs the model’s visual understanding and contributes to hallucination. To address this, we propose Semantic-Enhanced Visual Interpretation (SEVI), a method that guides the model’s attention toward the core components of semantic representations through a two-stage optimization process. Extensive experiments demonstrate that our approach significantly mitigates hallucinations.

While our method optimizes the attention distribution in LVLMs based on the underlying information flow, it does not directly enhance the flow mechanism itself. In future work, we plan to explore more efficient strategies for visual information propagation.

7 Limitation

Our method guides the model to focus on the most critical information, thereby reducing the occurrence of hallucinations. During our experiments, we observed a trade-off mechanism in the model’s focusing process: excessive focus leads to more conservative image captioning. In an effort to avoid hallucinated content, the model may overlook some details, which is reflected in a slight decrease in recall. Although our method demonstrates superior overall performance, showing a significant advantage on comprehensive metrics such as CAPTURE, it still faces a trade-off between reducing hallucinations and generating more details. To address this issue, we introduce hyperparameters to control the model’s level of conservativeness, allowing users to manually adjust the behavior based on specific application scenarios. Furthermore, as a training-free approach, our method offers greater usability but is inherently limited by the performance ceiling of the model itself.

References

- Samira Abnar and Willem H. Zuidema. 2020. [Quantifying attention flow in transformers](#). In *Proceedings of the 58th Annual Meeting of the Association for Computational Linguistics, ACL 2020, Online, July 5-10, 2020*, pages 4190–4197. Association for Computational Linguistics.
- Jinze Bai, Shuai Bai, Shusheng Yang, Shijie Wang, Sinan Tan, Peng Wang, Junyang Lin, Chang Zhou, and Jingren Zhou. 2023. [Qwen-vl: A versatile vision-language model for understanding, localization, text reading, and beyond](#). *Preprint*, arXiv:2308.12966.
- Shuai Bai, Keqin Chen, Xuejing Liu, Jialin Wang, Wenbin Ge, Sibao Song, Kai Dang, Peng Wang, Shijie Wang, Jun Tang, Humen Zhong, Yuanzhi Zhu, Mingkun Yang, Zhaohai Li, Jianqiang Wan, Pengfei Wang, Wei Ding, Zheren Fu, Yiheng Xu, and 8 others. 2025. [Qwen2.5-vl technical report](#). *Preprint*, arXiv:2502.13923.
- Cong Chen, Mingyu Liu, Chenchen Jing, Yizhou Zhou, Fengyun Rao, Hao Chen, Bo Zhang, and Chunhua Shen. 2025. [PerturboLLaVA: Reducing multimodal hallucinations with perturbative visual training](#). In *The Thirteenth International Conference on Learning Representations*.
- Wenliang Dai, Junnan Li, Dongxu Li, Anthony Meng Huat Tiong, Junqi Zhao, Weisheng Wang, Boyang Li, Pascale Fung, and Steven C. H. Hoi. 2023. [Instructblip: Towards general-purpose vision-language models with instruction tuning](#). In *Advances in Neural Information Processing Systems 36: Annual Conference on Neural Information Processing Systems 2023, NeurIPS 2023, New Orleans, LA, USA, December 10 - 16, 2023*.
- Anisha Gunjal, Jihan Yin, and Erhan Bas. 2024. [Detecting and preventing hallucinations in large vision language models](#). In *Thirty-Eighth AAAI Conference on Artificial Intelligence, AAAI 2024, Thirty-Sixth Conference on Innovative Applications of Artificial Intelligence, IAAI 2024, Fourteenth Symposium on Educational Advances in Artificial Intelligence, EAAI 2014, February 20-27, 2024, Vancouver, Canada*, pages 18135–18143. AAAI Press.
- Jinghan He, Kuan Zhu, Haiyun Guo, Junfeng Fang, Zhenglin Hua, Yuheng Jia, Ming Tang, Tat-Seng Chua, and Jinqiao Wang. 2024. [Cracking the code of hallucination in lvmms with vision-aware head divergence](#). *CoRR*, abs/2412.13949.
- Hongyu Hu, Jiyuan Zhang, Minyi Zhao, and Zhenbang Sun. 2023. [CIEM: contrastive instruction evaluation method for better instruction tuning](#). *CoRR*, abs/2309.02301.
- Ziwei Ji, Nayeon Lee, Rita Frieske, Tiezheng Yu, Dan Su, Yan Xu, Etsuko Ishii, Yejin Bang, Andrea Madotto, and Pascale Fung. 2023. [Survey of hallucination in natural language generation](#). *ACM Comput. Surv.*, 55(12):248:1–248:38.
- Seil Kang, Jinyeong Kim, Junhyeok Kim, and Seong Jae Hwang. 2025. [See what you are told: Visual attention sink in large multimodal models](#). *CoRR*, abs/2503.03321.
- Sicong Leng, Hang Zhang, Guanzheng Chen, Xin Li, Shijian Lu, Chunyan Miao, and Lidong Bing. 2024. [Mitigating object hallucinations in large vision-language models through visual contrastive decoding](#). In *IEEE/CVF Conference on Computer Vision and Pattern Recognition, CVPR 2024, Seattle, WA, USA, June 16-22, 2024*, pages 13872–13882. IEEE.
- Jiaming Li, Jiacheng Zhang, Zequn Jie, Lin Ma, and Guanbin Li. 2025. [Mitigating hallucination for large vision language model by inter-modality correlation calibration decoding](#). *CoRR*, abs/2501.01926.
- Tsung-Yi Lin, Michael Maire, Serge J. Belongie, James Hays, Pietro Perona, Deva Ramanan, Piotr Dollár, and C. Lawrence Zitnick. 2014. [Microsoft COCO: common objects in context](#). In *Computer Vision - ECCV 2014 - 13th European Conference, Zurich, Switzerland, September 6-12, 2014, Proceedings, Part V*, volume 8693 of *Lecture Notes in Computer Science*, pages 740–755. Springer.

- Fuxiao Liu, Kevin Lin, Linjie Li, Jianfeng Wang, Yaser Yacoob, and Lijuan Wang. 2024a. [Mitigating hallucination in large multi-modal models via robust instruction tuning](#). In *The Twelfth International Conference on Learning Representations, ICLR 2024, Vienna, Austria, May 7-11, 2024*. OpenReview.net.
- Hanchao Liu, Wenyuan Xue, Yifei Chen, Dapeng Chen, Xiutian Zhao, Ke Wang, Liping Hou, Rongjun Li, and Wei Peng. 2024b. [A survey on hallucination in large vision-language models](#). *CoRR*, abs/2402.00253.
- Haotian Liu, Chunyuan Li, Yuheng Li, and Yong Jae Lee. 2024c. Improved baselines with visual instruction tuning. In *Proceedings of the IEEE/CVF Conference on Computer Vision and Pattern Recognition (CVPR)*, pages 26296–26306.
- Haotian Liu, Chunyuan Li, Yuheng Li, Bo Li, Yuanhan Zhang, Sheng Shen, and Yong Jae Lee. 2024d. [Llava-next: Improved reasoning, ocr, and world knowledge](#).
- OpenAI, :, Aaron Hurst, Adam Lerer, Adam P. Goucher, Adam Perelman, Aditya Ramesh, Aidan Clark, AJ Ostrow, Akila Welihinda, Alan Hayes, Alec Radford, Aleksander Madry, Alex Baker-Whitcomb, Alex Beutel, Alex Borzunov, Alex Carney, Alex Chow, Alex Kirillov, and 401 others. 2024. [Gpt-4o system card](#). *Preprint*, arXiv:2410.21276.
- Anna Rohrbach, Lisa Anne Hendricks, Kaylee Burns, Trevor Darrell, and Kate Saenko. 2018. [Object hallucination in image captioning](#). In *Proceedings of the 2018 Conference on Empirical Methods in Natural Language Processing*, pages 4035–4045, Brussels, Belgium. Association for Computational Linguistics.
- Zhiqing Sun, Sheng Shen, Shengcao Cao, Haotian Liu, Chunyuan Li, Yikang Shen, Chuang Gan, Liangyan Gui, Yu-Xiong Wang, Yiming Yang, Kurt Keutzer, and Trevor Darrell. 2024. [Aligning large multimodal models with factually augmented RLHF](#). In *Findings of the Association for Computational Linguistics, ACL 2024, Bangkok, Thailand and virtual meeting, August 11-16, 2024*, pages 13088–13110. Association for Computational Linguistics.
- Gemini Team, Petko Georgiev, Ving Ian Lei, Ryan Burnell, Libin Bai, Anmol Gulati, Garrett Tanzer, Damien Vincent, Zhufeng Pan, Shibo Wang, Soroosh Mariooryad, Yifan Ding, Xinyang Geng, Fred Alcober, Roy Frostig, Mark Omernick, Lexi Walker, Cosmin Paduraru, Christina Sorokin, and 1118 others. 2024. [Gemini 1.5: Unlocking multimodal understanding across millions of tokens of context](#). *Preprint*, arXiv:2403.05530.
- Ashish Vaswani, Noam Shazeer, Niki Parmar, Jakob Uszkoreit, Llion Jones, Aidan N Gomez, Łukasz Kaiser, and Illia Polosukhin. 2017. Attention is all you need. *Advances in neural information processing systems*, 30.
- Bin Wang, Fan Wu, Xiao Han, Jiahui Peng, Huaping Zhong, Pan Zhang, Xiaoyi Dong, Weijia Li, Wei Li, Jiaqi Wang, and Conghui He. 2024a. [VIGC: visual instruction generation and correction](#). In *Thirty-Eighth AAAI Conference on Artificial Intelligence, AAAI 2024, Thirty-Sixth Conference on Innovative Applications of Artificial Intelligence, IAAI 2024, Fourteenth Symposium on Educational Advances in Artificial Intelligence, EAAI 2014, February 20-27, 2024, Vancouver, Canada*, pages 5309–5317. AAAI Press.
- Junyang Wang, Yuhang Wang, Guohai Xu, Jing Zhang, Yukai Gu, Haitao Jia, Jiaqi Wang, Haiyang Xu, Ming Yan, Ji Zhang, and Jitao Sang. 2024b. [Amber: An llm-free multi-dimensional benchmark for mllms hallucination evaluation](#). *Preprint*, arXiv:2311.07397.
- Lean Wang, Lei Li, Damai Dai, Deli Chen, Hao Zhou, Fandong Meng, Jie Zhou, and Xu Sun. 2023. [Label words are anchors: An information flow perspective for understanding in-context learning](#). In *Proceedings of the 2023 Conference on Empirical Methods in Natural Language Processing, EMNLP 2023, Singapore, December 6-10, 2023*, pages 9840–9855. Association for Computational Linguistics.
- Peng Wang, Shuai Bai, Sinan Tan, Shijie Wang, Zhihao Fan, Jinze Bai, Keqin Chen, Xuejing Liu, Jialin Wang, Wenbin Ge, Yang Fan, Kai Dang, Mengfei Du, Xuancheng Ren, Rui Men, Dayiheng Liu, Chang Zhou, Jingren Zhou, and Junyang Lin. 2024c. [Qwen2-vl: Enhancing vision-language model’s perception of the world at any resolution](#). *Preprint*, arXiv:2409.12191.
- Xintong Wang, Jingheng Pan, Liang Ding, and Chris Biemann. 2024d. [Mitigating hallucinations in large vision-language models with instruction contrastive decoding](#). In *Findings of the Association for Computational Linguistics, ACL 2024, Bangkok, Thailand and virtual meeting, August 11-16, 2024*, pages 15840–15853. Association for Computational Linguistics.
- Yike Wu, Yu Zhao, Shiwan Zhao, Ying Zhang, Xiaojie Yuan, Guoqing Zhao, and Ning Jiang. 2022. [Overcoming language priors in visual question answering via distinguishing superficially similar instances](#). In *Proceedings of the 29th International Conference on Computational Linguistics*, pages 5721–5729, Gyeongju, Republic of Korea. International Committee on Computational Linguistics.
- Guangxuan Xiao, Yuandong Tian, Beidi Chen, Song Han, and Mike Lewis. 2024. [Efficient streaming language models with attention sinks](#). In *The Twelfth International Conference on Learning Representations, ICLR 2024, Vienna, Austria, May 7-11, 2024*. OpenReview.net.
- Zhengyuan Yang, Linjie Li, Kevin Lin, Jianfeng Wang, Chung-Ching Lin, Zicheng Liu, and Lijuan Wang. 2023. [The dawn of llms: Preliminary explorations with gpt-4v\(ision\)](#). *Preprint*, arXiv:2309.17421.
- Qinghao Ye, Xianhan Zeng, Fu Li, Chunyuan Li, and Haoqi Fan. 2025. [Painting with words: Elevating](#)

- detailed image captioning with benchmark and alignment learning. In *The Thirteenth International Conference on Learning Representations*.
- Hao Yin, Guangzong Si, and Zilei Wang. 2025. [Clear-sight: Visual signal enhancement for object hallucination mitigation in multimodal large language models](#). *CoRR*, abs/2503.13107.
- Shukang Yin, Chaoyou Fu, Sirui Zhao, Tong Xu, Hao Wang, Dianbo Sui, Yunhang Shen, Ke Li, Xing Sun, and Enhong Chen. 2024. [Woodpecker: hallucination correction for multimodal large language models](#). *Sci. China Inf. Sci.*, 67(12).
- Bohan Zhai, Shijia Yang, Xiangchen Zhao, Chenfeng Xu, Sheng Shen, Dongdi Zhao, Kurt Keutzer, Manling Li, Tan Yan, and Xiangjun Fan. 2024. [Halle-switch: Rethinking and controlling object existence hallucinations in large vision-language models for detailed caption](#).
- Ce Zhang, Zifu Wan, Zhehan Kan, Martin Q. Ma, Simon Stepputtis, Deva Ramanan, Russ Salakhutdinov, Louis-Philippe Morency, Katia P. Sycara, and Yaqi Xie. 2025. [Self-correcting decoding with generative feedback for mitigating hallucinations in large vision-language models](#). *CoRR*, abs/2502.06130.
- Jianfei Zhao, Feng Zhang, Xin Sun, and Chong Feng. 2025. [Cross-image contrastive decoding: Precise, lossless suppression of language priors in large vision-language models](#). *Preprint*, arXiv:2505.10634.
- Yiyang Zhou, Chenhang Cui, Jaehong Yoon, Linjun Zhang, Zhun Deng, Chelsea Finn, Mohit Bansal, and Huaxiu Yao. 2024. [Analyzing and mitigating object hallucination in large vision-language models](#). In *The Twelfth International Conference on Learning Representations, ICLR 2024, Vienna, Austria, May 7-11, 2024*. OpenReview.net.
- Lanyun Zhu, Deyi Ji, Tianrun Chen, Peng Xu, Jieping Ye, and Jun Liu. 2024. [IBD: alleviating hallucinations in large vision-language models via image-biased decoding](#). *CoRR*, abs/2402.18476.
- Younan Zhu, Linwei Tao, Minjing Dong, and Chang Xu. 2025. [Mitigating object hallucinations in large vision-language models via attention calibration](#). *CoRR*, abs/2502.01969.

A Detailed Experiments

A.1 Benchmarks

We evaluate the performance of our method across three widely adopted multimodal hallucination benchmarks on the image captioning task. These include CHAIR, DetailCap, and AMBER.

CHAIR (Rohrbach et al., 2018) evaluates the proportion of hallucinated objects—those generated by the model but not present in the reference annotations. Following prior work, we randomly sample 500 images from the MSCOCO (Lin et al., 2014) dataset for evaluation. CHAIRs and CHAIRi are the main metrics to evaluate hallucination:

$$\begin{aligned} \text{CHAIR}_s &= \frac{|\text{Hallucinated Objects}|}{|\text{All Objects}|}, \\ \text{CHAIR}_i &= \frac{|\text{Hallucinated Sentences}|}{|\text{All Sentences}|} \end{aligned} \quad (7)$$

DetailCaps (Ye et al., 2025) is a fine-grained image captioning benchmark, accompanied by ground-truth detail captions generated by GPT-4V (Yang et al., 2023), Gemini 1.5 Pro (Team et al., 2024), and GPT-4o (OpenAI et al., 2024) for evaluation purposes. It comprises 4,870 images from various datasets; we use a subset of 700 images from MSCOCO in our experiments. CAPTURE evaluates the alignment between generated and reference captions by computing F1 scores using both hard and soft matching across three semantic aspects: entities ($F1_{\text{obj}}$), attributes ($F1_{\text{attr}}$), and relations ($F1_{\text{rel}}$). The final score is calculated as a weighted average:

$$\text{CAPTURE} = \frac{\alpha F1_{\text{obj}} + \beta F1_{\text{attr}} + \gamma F1_{\text{rel}}}{\alpha + \beta + \gamma} \quad (8)$$

where $\alpha = 5$, $\beta = 5$, and $\gamma = 2$.

AMBER (Wang et al., 2024b) contains 1,004 carefully curated high-quality images, each with manually annotated objects. AMBER contains multiple evaluation metrics: *CHAIR*, *Cover*, *Hal*, and *Cog*. Given a list of annotated objects $A_{\text{obj}} = \text{obj}_1^A, \text{obj}_2^A, \dots, \text{obj}_n^A$ and a set of generated ob-

jects R'_{obj} , each metric is defined as follows:

$$\begin{aligned} \text{CHAIR} &= 1 - \frac{\text{len}(R'_{\text{obj}} \cap A_{\text{obj}})}{\text{len}(R'_{\text{obj}})}, \\ \text{Cover} &= \frac{\text{len}(R'_{\text{obj}} \cap A_{\text{obj}})}{\text{len}(A_{\text{obj}})}, \\ \text{Hal} &= \frac{|\text{CHAIR} > 0|}{|\text{All Captions}|}, \\ \text{Cog} &= \frac{\text{len}(R'_{\text{obj}} \cap H_{\text{obj}})}{\text{len}(R'_{\text{obj}})} \end{aligned} \quad (9)$$

where H_{obj} denotes the set of hallucinated target objects generated by LVLMs, and All Captions refers to the total number of generated captions.

A.2 Baselines

We conduct a comparison between our method and several SOTA de-hallucination techniques:

- **VCD** (Leng et al., 2024) introduces Gaussian noise into images to activate language priors, thereby constructing negative contexts and removing these priors through contrastive decoding. However, this approach leads to a loss of visual information. Moreover, the use of noisy images deviates from the model’s training distribution, potentially causing performance degradation.
- **ICD** (Wang et al., 2024d) constructs negative contexts by designing adversarial instructions and applies contrastive decoding to mitigate their influence. Like VCD, it faces challenges such as visual information loss and performance bias.
- **IBD** (Zhu et al., 2024) strengthens the model’s focus on visual information by using the original context as a negative reference, and further refines contrastive decoding via inter-layer and inter-context consistency mechanisms.
- **VAR** (Kang et al., 2025) reallocates attention from sink visual tokens to other visual tokens, allowing the model to capture more detailed visual information.
- **VAF** (Yin et al., 2025) rebalances the attention allocation between instructions and visual inputs, redirecting attention from the textual instructions toward the visual information.

Setting	Cs↓	Ci↓	R↑	R-Cs-Ci↑
$\kappa = 0.15$	21.6	7.1	57.6	28.9
$\kappa = 0.2$	17.8	5.5	56.9	33.6
$\kappa = 0.25$	12.6	6.3	49.1	30.2
$\kappa = 0.3$	11.0	5.4	44.8	28.4

Table 6: Explore on hyperparameter κ with the *Focused* mode.

- **DeFG** (Zhang et al., 2025) generates negative contexts via cross-modal back-translation and strengthens consistency signals throughout the contrastive decoding process.
- **CICD** (Zhao et al., 2025) leverages the consistency of language priors across images by using different images to construct negative contexts. It detects harmful priors via consistency analysis and removes them through contrastive decoding, while retaining beneficial priors essential for accurate understanding.

A.3 Hyperparameters

We investigate the appropriate setting of hyperparameters using LLaVA-1.5-7B. The parameter κ serves as the threshold for distinguishing between core semantic heads and global semantic heads. We analyze the peak attention values of semantic heads, as shown in Fig. 6. Based on this analysis, we explore the impact of κ under the focused mode, with the results presented in Tab.6. A higher threshold encourages the model to attend to more central information, resulting in a lower hallucination rate but also a reduced recall. To balance these trade-offs, we define a heuristic metric to evaluate the model’s overall performance. Based on the experimental results, we set $\kappa = 0.2$.

The attention adjustment strength ω and the starting layer (SL) for attention optimization are interdependent. Therefore, we perform a joint search over these two hyperparameters, with the results summarized in Tab.7. Based on two heuristic evaluation metrics, we select two representative hyperparameter configurations, corresponding to the Focused mode ($\omega=4$, SL=5) and Balanced modes ($\omega=0.5$, SL=9).

B Case Study

To demonstrate the effectiveness of our method in mitigating hallucinations, we provide qualitative case studies. We select one simple image (Fig. 7)

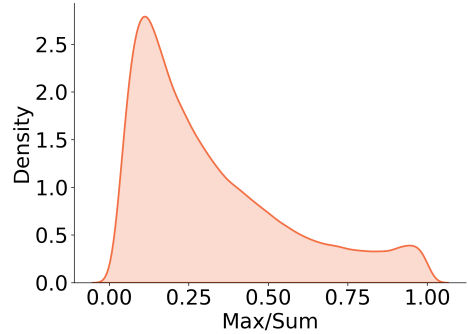


Figure 6: Semantic attention peaks. We plot the KDE (Kernel Density Estimation) of the peak attention weights for attention heads focusing on semantic representations. The x-axis represents the proportion of the highest-attended representation’s attention weight among all semantic representations, while the y-axis denotes the density.

and one complex image (Fig. 8) as case studies. The captions were generated by LLaVA-1.5, with hallucinated content highlighted in red and image-consistent content highlighted in green.

It can be observed that Regular Decoding produces a large amount of hallucinated content, even in the simple image. In contrast, our method effectively reduces the occurrence of such hallucinations. Both the Focused and Balanced modes significantly mitigate hallucinations; however, the Focused mode makes the model overly conservative, potentially overlooking fine-grained details. For example, in Fig. 8, the Focused mode fails to capture items such as *knife* and *fork*, whereas the Balanced mode not only reduces hallucinations but also preserves more detailed information.

Setting	CHAIRs↓	CHAIRi↓	Recall ↑	R-Cs-Ci↑	2R-Cs-Ci↑
$\omega=0.5, SL=2$	32.8	8.7	68.0	26.5	94.5
$\omega=0.5, SL=5$	34.4	9.4	68.8	25.0	93.8
$\omega=0.5, SL=9$	31.4	9.1	67.8	27.3	95.1
$\omega=0.5, SL=17$	45.2	12.3	74.3	16.8	91.1
$\omega=1, SL=2$	29.4	7.7	64.4	27.3	91.7
$\omega=1, SL=5$	27.4	8.0	64.7	29.3	94.0
$\omega=1, SL=9$	26.0	6.7	63.7	31.0	94.7
$\omega=1, SL=17$	47.0	13.5	74.3	13.8	88.1
$\omega=2, SL=2$	23.4	7.3	60.5	29.8	90.3
$\omega=2, SL=5$	23.6	6.7	59.9	29.6	89.5
$\omega=2, SL=9$	23.6	7.1	61.2	30.5	91.7
$\omega=2, SL=17$	47.8	13	74.9	14.1	89.0
$\omega=4, SL=2$	18.0	6.1	55.5	31.4	86.9
$\omega=4, SL=5$	17.8	5.5	56.9	33.6	90.5
$\omega=4, SL=9$	21.6	7.1	57.6	28.9	86.5
$\omega=4, SL=17$	47.0	13.0	74.1	14.1	88.2

Table 7: Results of grid search. *SL* stands for *Start Layer*, indicating the layer from which attention optimization begins. *Cs*, *Ci*, and *R* separately represent *CHAIRs*, *CHAIRi*, and *Recall*.



Regular

The image features a red fire hydrant sitting in the middle of a field with its base elevated up in the sand. The fire hydrant is surrounded by plants and likely serves its purpose in case of emergencies. It is situated near a concrete wall which appears to be a part of the surrounding landscaping. The hydrant is prominently visible in the scene, with no other objects or potted plants providing a sense of perspective within the area.

Balanced mode

The image features a red fire hydrant prominently sitting in a rock bed or rock garden. The hydrant is situated on a gravel bed and is surrounded by green plants and shrubs. The vibrant red fire hydrant stands out against the lush greenery, creating a harmonious blend of colors and textures. The combination of the vivid red hue and the lush plant life creates a serene and peaceful atmosphere.

Focused mode

The image features a red fire hydrant sitting in a rock bed or gravel in front of some plants and bushes. The fire hydrant is red in color, and its bright red hue contrasts sharply with the surrounding plants, adding a beautiful contrast to the garden scene. The bright red color of the fire hydrant creates a striking contrast with its surroundings, making it a striking addition to the scene.

Figure 7: Case study I.



Regular

The image shows a middle-aged couple seated together at a dining table, enjoying a meal. In front of them, several bowls are filled with food, and wine glasses are positioned around the table. Other tableware items include a fork, knife, and spoons, placed near the people. The couple appears to be sitting in a casual restaurant setting. Additionally, there is a chair on the right side of the table for another person, although no one else is visible in the scene. A person can be seen in the background, possibly a waiter or a fellow patron at the restaurant.

Balanced mode

The image depicts an older couple sitting together at a dining table, enjoying a meal of soup and salad. They have multiple plates, cups, and bowls filled with food in front of them. Various utensils such as forks, spoons, and knives can be seen placed on the table, ready for use. Additional tableware is present, including a vase, and a bottle can be spotted on the table. The couple seems to be enjoying each other's company and sharing the dining experience.

Focused mode

The image shows two elderly people, a man and a woman, sitting at a dining table and enjoying a meal together. They appear to be smiling while posing for the camera. On the table, there are various bowls containing different types of food, along with multiple spoons placed in and around them. Additionally, there are several wine glasses on the table, indicating a variety of wines may have been served with the meal. Overall, it's a joyful and happy moment.

Figure 8: Case study II.